Optics Letters

Frequency-modulated continuous-wave laser ranging using low-duty-cycle signals for the applications of real-time super-resolved ranging

Zhongyang Xu,† Xiuyuan Sun,† Fengxi Yu, Kai Chen, and Shilong Pan*

Key Laboratory of Radar Imaging and Microwave Photonics, Ministry of Education, Nanjing University of Aeronautics and Astronautics, Nanjing 210016, China
**Corresponding author: pans@nuaa.edu.cn*

Received 12 October 2020; revised 24 November 2020; accepted 28 November 2020; posted 2 December 2020 (Doc. ID 412262); published 7 January 2021

A frequency-modulated continuous-wave laser ranging method using low-duty-cycle linear-frequency-modulated (LFM) signals is proposed. A spectrum consisting of a dense Kronecker comb is obtained so that the frequency of the beat signal can be measured with finer resolution. Since the dense comb is provided, super-resolved laser ranging can be achieved using a single-parametric frequency estimation method. Therefore, the run times of the estimation are reduced which promises real-time applications. A proof-of-concept experiment is carried out, in which an LFM signal with a bandwidth of 5 GHz and a duration of 1 μs is used. The duty-cycle of the LFM signal is 10%. The time delay of a scanning variable optical delay line is obtained in real time from the frequency of the highest comb tooth, of which the measurement resolution is 20 ps. Moreover, a single-parametric nonlinear least squares method is used to fit the envelope so that the time delay can be estimated with super-resolution. The standard deviation of the estimation displacements is 2.3 ps, which is 87 times finer than the bandwidth-limited resolution (200 ps). Therefore, the variation of the time delay can be precisely monitored. The proposed method may be used to achieve real-time high-resolution laser ranging with low-speed electronic devices.

https://doi.org/10.1364/OL.412262

Frequency-modulated continuous-wave (FMCW) laser ranging uses a linear-frequency-modulated (LFM) or swept-frequency laser as the light source [1], which has been widely used in optical coherence tomography (OCT) [2], FMCW lidar [3,4], and optical frequency domain reflectometry (OFDR) [5]. In the receiver of an FMCW laser ranging system, Fourier transforms are always used in signal processing to extract the distance information. The distance can be extracted from the position of the compressed pulse [6,7] or obtained from the frequency of the beat signal [8]. According to the principle of Fourier transforms, the resolution of an FMCW laser ranging system is limited by the bandwidth of the swept-frequency light. The resolution is equal to c/B, in which c is the speed of light in a vacuum, and B is the bandwidth of the lightwave [3]. Therefore, a large bandwidth is required to achieve high-resolution FMCW laser ranging [9]. However, the large bandwidth usually calls for high-speed electronic devices, such as wideband transmitters and receivers which enhance the cost of an FMCW laser ranging system. Moreover, it is difficult to achieve perfectly linear swept frequency in a large range. Additional linearization methods are demanded to correct the frequency distortions for a swept-frequency laser [10,11]. Therefore, it is significant for an FMCW laser ranging system to achieve a high resolution using a small bandwidth [12].

Super-resolution is the method that can estimate the optical path length with a resolution finer than the bandwidth-limited resolution (c/B) [13,14]. For the FMCW ranging system using optical de-chirping, frequency estimation methods [15–17] can be used to estimate the beat frequency with low uncertainties. The 2σ uncertainties can be as low as $10^{-4} - 10^{-5}$ of Fourier transform-limited resolution. But the sophisticated algorithms are time-inefficient so that real-time super-resolution FMCW laser ranging is difficult to achieve. Other methods can also improve the measurement performance, such as zero-filling [18] and Fourier transforms reordering [6]. They are essentially interpolation methods, in which the spectra are sampled with high sampling rates so that the resolution of the spectra can be improved. The computation of the interpolation methods is much less than super-resolution algorithms so that real-time applications may be achieved [6]. Moreover, the interpolation methods provide highly interpolated results which is helpful to further improve the performance of super-resolution algorithms (Richardson–Lucy deconvolution) [14].

In this Letter, we propose an FMCW laser ranging method using a low-duty-cycle LFM in which all-optical zero-filling is achieved. A beat signal consisting of dense frequency comb teeth is generated so that the frequency of the beat signal can be measured with low uncertainty. A proof-of-concept experiment is carried out, in which an LFM signal with a 5-GHz bandwidth and a 10% duty cycle is used. The time delay of a variable-optical-delay-line (VODL) is real-time measured with a resolution step of 20 ps, which is 10 times finer than the bandwidth-limited resolution (200 ps). Moreover, since the

dense comb teeth provide more valid points to fit the envelope of the comb teeth, a single-parametric NLS fitting method can be used to achieve super-resolved ranging with short run time. In the experiment, the standard deviation of the estimation displacements for the NLS method can be further reduced to 2.3 ps. A signal with a time length of 1.9 s is analyzed. The run time for the analysis is less than 1.5 s. The method can be used for real-time high-resolution FMCW laser ranging with low-speed electronic devices.

In an FMCW laser ranging system, an LFM lightwave is always used as the probe lightwave. In the receiver, the probe lightwave beats with the local lightwave in a photodetector, which generates a beat signal as

$$I(t) = \eta \cos(2\pi f_{\text{beat}} t - \phi), \tag{1}$$

where $f_{\text{beat}} = B\tau/T$, τ is the time delay of the probe lightwave, ϕ is a constant phase, η is the responsibility of the photodetector, and B and T are the bandwidth and the duration of the modulation signal, respectively. Discrete Fourier transform (DFT) is always used to extract the time delay. The obtained spectrum of the beat signal has a peak centered at the beat frequency (f_{beat}), if the time length of the sampled signal is shorter than the duration of the LFM signal. The ability to resolve multiple targets depends on the width of the peak. But, the measurement resolution for a single target depends on the frequency resolution of the spectrum which is determined by the DFT bin size [13]. To improve the resolution of the time delay, the time length of the sampled signal can be increased to reduce the DFT bin size.

However, if the time length of the sampled signal is increased to be longer than the duration of the LFM signal, a repeating LFM signal is actually used in the system, of which the spectrum consists of a Kronecker comb [19]. The frequency interval between the comb teeth is proportional to the inverse of the period, which can be given by

$$S(f_n) \propto \left\{ \frac{1}{T-\tau} \text{sinc}[(T-\tau)(f_n - f_{\text{beat}})] \right\}^2, \tag{2}$$

where n is an integer and $f_n = n/T$ is the frequency of the nth comb tooth. The envelope of the comb teeth is a square of sinc function with a sampling interval of $1/T$. The measured beat frequency can only be the frequency of the comb teeth (f_n). However, in practice, the frequency of the beat signal is unlikely to equal to f_n. The exact beat frequency can be expressed as

$$f_{\text{beat}} = (n + \delta n)\frac{1}{T}, \tag{3}$$

which means that the beat frequency is centered some fraction δn of the way between comb teeth. For the ranging of multiple targets, the bandwidth-limited resolution of different targets is c/B, which is calculated according to the width of the envelope. But for the ranging of the single target, the measurement resolution of the time delay depends on the sampling interval of the envelope. Therefore, if the sampling interval of the envelope can be reduced, the measurement uncertainty can be reduced. An easy approach to obtain a highly interpolated envelope is to use a low-duty-cycle LFM signal. Using an LFM signal with a duty cycle α, the repeating period is enlarged by $1/\alpha$ times. The frequency of the beat signal can be expressed as

$$f'_{\text{beat}} = (n + \delta n)\frac{\alpha}{T}. \tag{4}$$

It is obvious that the frequency interval can be reduced to α/T so that the measurement uncertainty may be reduced by $1/\alpha$ times. It should be noted that the improvement of performance only depends on the duty cycle. The method can be used for signals with different periods so long as the frequency interval is larger than the linewidth of a comb tooth. Moreover, using low-duty-cycle signals, all-optical zero-filling is achieved without complicated digital processing methods, which promises real-time applications of high-resolution FMCW laser ranging.

To further reduce the measurement uncertainty of FMCW laser ranging, the value of δn has to be determined. Using frequency estimation methods, the spectrum shown in Eq. (2) can be well fitted so that the beat frequency can be estimated with super-resolution. However, since multiple parameters are required to be estimated, the run times are too long to achieve real-time super-resolved ranging, which can be more than 100 s for the NLS methods [13].

Nevertheless, it should be noted that the time delay only impacts the envelope of the comb. According to Eq. (2), the envelope is a single-parameter function in which only the time delay (τ) is required to be estimated. Therefore, the run times of the NLS fitting methods can be largely reduced. However, in a traditional FMCW laser ranging system, a 100% duty-cycle LFM signal is used indicating a frequency interval of $1/T$. As a result, there is only one comb tooth in the main lobe which makes it difficult to precisely estimate the center frequency. Using a low-duty-cycle LFM signal, multiple comb teeth are included in the main lobe so that the envelope can be sampled with a high rate, which makes it possible to estimate the fraction δn with a single-parametric NLS method. Finally, the time delay can be fast estimated with resolution finer than the bandwidth-limited resolution. The proposed scheme is a kind of interpolation method, of the sort which have been used to improve the resolution of time delay. The significance of the proposed method is that no complicated post-processing method is used for interpolation. The highly interpolated envelope makes it feasible to implement fast super-resolved ranging via a single-parametric NLS method.

Figure 1 is the schematic diagram of the proof-of-concept experiment system. An LFM with a bandwidth of 5 GHz and a duration of 1 μs is used to modulate the lightwave in a Mach–Zehnder modulator (Fujitsu FTM 7938). The beat signal is detected by a balanced photodetector (BPD) (Thorlabs 480C), and observed by an electrical spectrum analyzer (ESA). The time delay of the probe lightwave is changed using a VODL. The spectra of beat signals are shown in Fig. 2. In Fig. 2(a), the duty cycle is 100% so that the frequency interval between the comb teeth is 1 MHz. As a result, in the top three subfigures of Fig. 2(a), the frequencies of the highest comb tooth are all 87 MHz even though the time delay is changed by 120 ps. In Fig. 2(b) the duty cycle is 10%. The frequency interval between the comb teeth is 100 kHz so that small changes of the time delay can be observed. In the top three subfigures of Fig. 2(b), the frequencies of the highest comb tooth are 87.2 MHz, 86.9 MHz, and 86.6 MHz, respectively. Figure 2(c) shows the time delay measured from the frequency of the highest comb tooth. The measured results using a 100% duty cycle signal shows an obvious step-resolution of 200 ps, while it is 20 ps for a 10% duty cycle. It should be noted that the width of the envelope of the comb teeth (gray lines) is not changed, which is determined by the bandwidth of 5 GHz. It is only the sampling rate that is increased. As a result, two adjunct targets, between

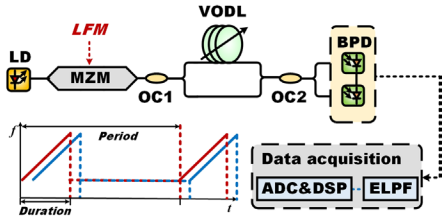

Fig. 1. Schematic diagram of the proof-of-concept system. LD: laser diode; MZM: Mach–Zehnder modulator; LFM: linear-frequency-modulated signal; OC: optical coupler; VODL: varied optical delay line. BPD: balanced photodetector; ELPF: electrical low pass filter; ADC: analog-to-digital convertor. DSP: digital signal processor. The low-duty-cycle LFM signal is shown in the subfigure.

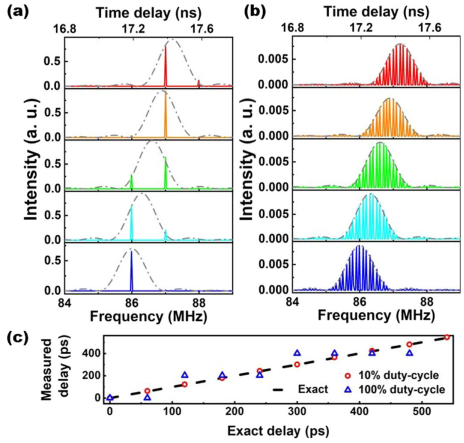

Fig. 2. Measured spectra at different time delays. The duty cycle o is (a) 100% and (b) 10%. (c) Measured and the exact time delays.

which the difference of time delay is less than $1/B$, can still not be resolved. But, for a single target, the time delay can be measured with a resolution finer than 1/B, since the frequency interval is reduced.

The time delay is also continuously changed using the scanning VODL. The beat signals are recorded by an oscilloscope with a sampling rate of 250 MHz and processed by DFT to obtain the spectra. Figure 3 shows the obtained spectrograms. The time length of the recorded beat signal is around 1.9 s and the length of the DFT window is around 20 μs, which includes 2 periods of the low-duty cycle LFM signal. The frequency has been converted to the time delay. In Figs. 3(a) and 3(b), the time delay linearly scans with a speed of 128 ps/s, while it vibrates in Figs. 3(c) and 3(d). In Fig. 3(a), since LFM signals with a 100% duty cycle are used, only two values (17.4 ns and 17.6 ns) are obtained, which cannot depict the linear changes of the time delay. However, using the LFM with a 10% duty cycle, the linear changes of the time delay are clearly shown in Fig. 3(b). For the vibrating VODL, the time delay continually changes in a range of 100 ps. But in Fig. 3(c), the measured time delay jitters between 17.2 ns and 17.4 ns. In Fig. 3(d), using the proposed method, the smooth vibration of the time delay can be observed. Moreover, since the low-duty-cycle LFM signals are used, no post-processing methods are demanded. The time delays can be directly monitored in real time based on the instantaneous spectra. In Visualization 1 and Visualization 2, the real-time spectra measured by the ESA are shown. The vibration in a

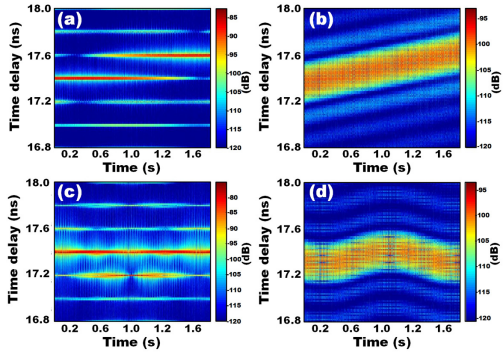

Fig. 3. Measured spectrogram for a scanning VODL. (a)–(b) The time delay linearly scans with a speed of 128 ps/s. (c)–(d) The time delay vibrates in a range of 100 ps. The duty cycle is 100% in (a) and (c), while it is 10% in (b) and (d). The real-time monitoring of the vibration can be seen in Visualization 1 and Visualization 2.

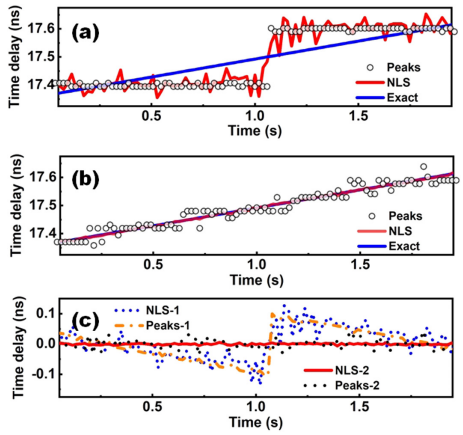

Fig. 4. (a)–(b) Measured (black circles) and estimated (red lines) time delays at different times in Figs. 3(a) and 3(b). (c) Displacements between the measured (or estimated) and exact results.

range of 200 ps is clearly visualized using a 10% duty cycle (see Visualization 2).

To further reduce the measurement uncertainty, a single-parametric NLS method is used to estimate the center frequency of the envelope with super-resolution. The envelopes of the comb teeth at different times in Figs. 3(a) and 3(b) are fitted with a sinc function so that the time delay can be estimated, which is shown with red lines in Figs. 4(a) and 4(b). Meanwhile, the time delays in Figs. 3(a) and 3(b) are also measured from the frequencies of the highest comb teeth, which are shown with black circles in Fig. 4. In every 20 ms, a beat signal with a time-length of 20 μs is used to obtain the instantaneous spectra. It can be seen that the step-resolution in Fig. 4(b) is reduced to 20 ps. Moreover, in Fig. 4(a), the estimation errors are still large and there is still a resolution step. However, in Fig. 4(b), the estimation errors are significantly reduced so that the estimated results (red line) match well with the exact time delay (blue line). It is because the envelopes of the frequency comb teeth are sampled with high sampling rates using low-duty-cycle signals. The highly interpolated envelopes make it feasible to estimate the time delay using the single-parametric NLS method.

Moreover, Fig. 4(c) shows the measurement and estimation displacements. For the signals with a 100% duty cycle,

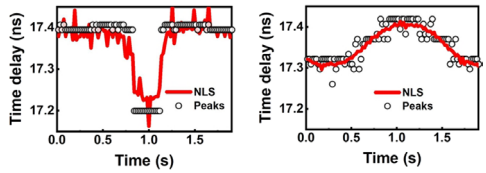

Fig. 5. Measured (black circles) and estimated (red lines) time delays at different times of Figs. 3(c) and 3(d).

the standard deviations of the measurement (Peaks-1) and estimation (NLS-1) displacements are 52.3 ps and 52.0 ps, which means that the single-parametric NLS method does not work for 100% duty cycle signals. However, for signals with a 10% duty cycle, the standard deviations of the measurement (Peaks-2) and estimation (NLS-2) displacements are 17.7 ps and 2.3 ps. The standard deviation of NLS-2 is reduced to around 87 times smaller than the bandwidth-limited resolution. Besides, Fig. (5) shows the measured and estimated time delays for a vibrating VODL. The time delay vibrates in a range of 100 ps. But, in Fig. 5(a), the estimated time delays still jitter in a range of 180 ps, and there is still a resolution step. In Fig. 5(b), using low-duty-cycle signals, the measured time delays continuously change with a small step, and the estimated results clearly show a smooth vibration between 17.3 ns and 17.4 ns, which matches well with the actual vibration.

To demonstrate the real time of the proposed method, the run time of the single-parameter NLS method is analyzed in detail. The total time length of the sampled beat signal is around 1.9 s. To shorten the run times, a beat signal with a time length of 40 μs in every 40 ms is used for DFT. The envelope of the dense comb teeth is further interpolated to reduce the estimation errors. The interpolation numbers are, respectively, 2, 5, 10, and 100 for the lines in Fig. 6. The estimation errors reduce with the increase of the interpolation number, while the run time also increases. If the interpolation number is 10, the run time of the estimation is 1.48 s, which is less than the time length of the beat signal (1.9 s). Meanwhile, the estimation errors are small enough for super-resolution ranging. In practice, the frame rate of the ESA is several hertz. It is feasible to process the measured spectrum with the single-parameter NLS method in real time. Therefore, the proposed method promises a quasi-real-time super-resolved ranging even though the measurement uncertainty is not as good as the previous works. In addition, the single-parametric NLS method cannot be used to super-resolve adjunct targets. The super-resolution in this work means that the method can extract the time delay of a single target with a resolution finer than 1/B. In the experiment, the largest measured time delay is 1 μs, which can be further enhanced using long-duration signals. Although it may be difficult to generate a 1μs signal with a bandwidth of 5 GHz, it is easier to reduce the duration from 10 μs to 1 μs than to enhance the bandwidth

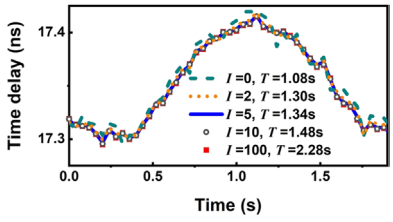

Fig. 6. Estimated time delays using different interpolation numbers (I). T is the run time. The time length of the signal is 1.9 s.

from 5 GHz to 50 GHz. Therefore, it is affordable to use short signals since the improvement of resolution is remarkable.

In conclusion, we propose a super-resolution method for real-time FMCW laser ranging. Since low-duty-cycle LFM signals are used, the frequency interval between the comb teeth is reduced. As a result, it is feasible to estimate the time delay with super-resolution using a single-parametric NLS fitting method. An LFM with 5GHz bandwidth and a 10% duty-cycle is used. The time delay of a scanning VODL can be directly monitored from the real-time spectra of the beat signal with a step-resolution of 20 ps, which is 10 times finer than the bandwidth-limited resolution. Using the single-parametric NLS method, the standard deviation of the estimation displacements can be reduced to 2.3 ps, which is 87 times smaller than the bandwidth-limited resolution. Moreover, since there is only one parameter required in the NLS method, the run time is largely reduced. Therefore, the proposed method can be used to achieve real-time super-resolved FMCW laser ranging.

Funding. National Natural Science Foundation of China (61605190); Shanghai Academy of Spaceflight Technology Innovation Fund (SAST2018054); Project of Key Laboratory of Radar Imaging and Microwave Photonics (RIMP2020001).

Disclosures. The authors declare no conflicts of interest.

†These authors contributed equally to this Letter.

REFERENCES

1. M. C. Amann, T. Bosch, M. Lescure, R. Myllyla, and M. Rioux, Opt. Eng. **40**, 10 (2001).
2. T. DiLazaro and G. Nehmetallah, Opt. Express **26**, 2891 (2018).
3. J. Anderson, R. Massaro, J. Curry, R. Reibel, J. Nelson, and J. Edwards, Photogramm. Eng. Remote Sens. **83**, 721 (2017).
4. J. Riemensberger, A. Lukashchuk, M. Karpov, W. Weng, E. Lucas, J. Liu, and T. J. Kippenberg, Nature **581**, 164 (2020).
5. H. Ghafoori-Shiraz and T. Okoshi, Opt. Lett. **10**, 160 (1985).
6. J. F. Campbell, B. Lin, A. R. Nehrir, F. W. Harrison, and M. D. Obland, Opt. Lett. **39**, 6078 (2014).
7. J. Clement, C. Schnébelin, H. G. de Chatellus, and C. R. Fernández-Pousa, Opt. Express **27**, 12000 (2019).
8. P. Adany, C. Allen, and R. Hui, J. Lightwave Technol. **27**, 3351 (2009).
9. Z. Lu, T. Yang, Z. Li, C. Guo, Z. Wang, D. Jia, and C. Ge, Opt. Lett. **43**, 4144 (2018).
10. X. Zhang, J. Pouls, and M. C. Wu, Opt. Express **27**, 9965 (2019).
11. T. Zhang, X. Qu, and F. Zhang, Opt. Express **26**, 11519 (2018).
12. N. Kuse and M. E. Fermann, APL Photon. **4**, 106105 (2019).
13. M. I. Bodine and R. R. McLeod, Opt. Lett. **41**, 159 (2016).
14. J. F. Campbell, B. Lin, A. R. Nehrir, F. W. Harrison, and M. D. Obland, Opt. Lett. **39**, 6981 (2014).
15. R. Roy and T. Kailath, IEEE Trans. Acoust. Speech Signal Process. **37**, 984 (1989).
16. P. Stoica and A. Nehorai, IEEE Trans. Acoust. Speech Signal Process. **37**, 720 (1989).
17. E. D. Moore and R. R. McLeod, Opt. Express **19**, 8117 (2011).
18. C. Dorrer, N. Belabas, J. Likforman, and M. Joffre, J. Opt. Soc. Am. B **17**, 1795 (2000).
19. A. Nehorai and B. Porat, IEEE Trans. Acoust. Speech Signal Process. **34**, 1124 (1986).